An Ancient Fecundability-Associated Polymorphism Switches a Repressor into an Enhancer of Endometrial *TAP2* Expression

Katelyn M. Mika[1] and Vincent J. Lynch[1,*]

Variation in female reproductive traits, such as fertility, fecundity, and fecundability, is heritable in humans, but identifying and functionally characterizing genetic variants associated with these traits has been challenging. Here, we explore the functional significance and evolutionary history of a T/C polymorphism of SNP rs2071473, which we have previously shown is an eQTL for *TAP2* and significantly associated with fecundability (time to pregnancy). We replicated the association between the rs2071473 genotype and *TAP2* expression by using GTEx data and demonstrated that *TAP2* is expressed by decidual stromal cells at the maternal-fetal interface. Next, we showed that rs2071473 is located within a progesterone-responsive *cis*-regulatory element that functions as a repressor with the T allele and an enhancer with the C allele. Remarkably, we found that this polymorphism arose before the divergence of modern and archaic humans, segregates at intermediate to high frequencies across human populations, and has genetic signatures of long-term balancing selection. This variant has also previously been identified in genome-wide association studies of immune-related disease, suggesting that both alleles are maintained as a result of antagonistic pleiotropy.

Introduction

Variation in female reproductive traits, such as age of menarche and menopause, fertility, age at first and last birth, fecundity, and fecundability, is heritable in humans.[1,2] However, identifying the genetic bases for variation in most of these traits has proven challenging because of limited sample sizes, strong gene-environment interactions,[1–3] widespread contraceptive use, and significant clinical heterogeneity among infertile couples. For example, although genome-wide association studies (GWASs) have identified loci associated with age of menarche and menopause[4–9] and age at first and last birth,[10] few studies have successfully identified genetic variants associated with fertility, fecundity, and fecundability.[3,10–12]

We recently performed an integrated expression quantitative trait locus (eQTL) mapping and association study to identify mid-secretory endometrial eQTLs that influence pregnancy outcomes in a prospective study of Hutterite women.[13–15] Among the 189 eQTLs we identified, two were also associated with fecundability (time to pregnancy).[15] The most significant association was rs2071473 ($p = 1.3 \times 10^{-4}$), an eQTL associated with expression of *TAP2* (transporter 2, ATP binding cassette subfamily B member [MIM: 170261]) in the human leukocyte antigen (HLA) class II region. The C allele of rs2071473 was associated with longer intervals to pregnancy and higher expression of *TAP2* in mid-secretory-phase (receptive) endometrium. The median time to pregnancy, for example, was 2.0, 3.1, and 4.0 months among women with the TT, CT, and CC genotypes, respectively.[15]

An essential step in implantation is the establishment of receptivity by the hormone-primed endometrium. This "window of implantation" occurs in the mid-secretory phase of the menstrual cycle,[16] after endometrial stromal fibroblasts (ESFs) have differentiated (decidualized) into decidual stromal cells (DSCs) in response to progesterone and cyclic-AMP (cAMP).[17,18] Decidualization underlies a suite of molecular, cellular, and physiological responses, including maternal immunotolerance of the fetal allograft, that support pregnancy.[18,19] Although the function of TAP2 in the decidualized endometrium and the process of implantation have not been elucidated, TAP2 plays an integral role in translocating peptides from the cytosol to major histocompatibility complex (MHC) class I molecules in the endoplasmic reticulum.[20] These data suggest that TAP2-dependent antigen processing and presentation by DSCs play a role in establishing receptivity to implantation and immunotolerance at the maternal-fetal interface, most likely by modifying the interactions between DSCs and immune cells in the decidualized endometrium.[21]

Here, we explore the functional significance and evolutionary history of the rs2071473 T/C polymorphism. We first replicate the association between the rs2071473 genotype and *TAP2* expression by using Genotype-Tissue Expression (GTEx) data and then demonstrate that *TAP2* is expressed by DSCs at the maternal-fetal interface. Next, we show that rs2071473 is located within a cAMP- and progesterone-responsive regulatory element and disrupts a putative DDIT3 (CHOP10) binding site that functions as a repressor with the rs2071473 T allele and an enhancer with the C allele. Remarkably, we found that the T/C polymorphism arose before the divergence of modern and archaic humans, segregates at intermediate to high frequencies across human populations, and has genetic signatures of long-term balancing selection.

[1]Department of Human Genetics, University of Chicago, 920 East 58th Street, CLSC 319C, Chicago, IL 60637, USA
*Correspondence: vjlynch@uchicago.edu
http://dx.doi.org/10.1016/j.ajhg.2016.09.002.

Material and Methods

rs2071473 Is a Multi-tissue eQTL for *TAP2*, *HLA-DOB*, and *HLA-DRB6*

We replicated the association between the T/C polymorphism at rs2071473 and *TAP2* expression levels by using GTEx data (dbGaP: phs000424.v6.p1) for 35 tissues, including the uterus.[22,23] We also used GTEx data to identify other genes for which rs2071473 was an eQTL. In breif, we queried the GTEx Portal by using the "Single Tissue eQTLs" search form for SNP rs2071473.

TAP2 Is Produced by DSCs at the Maternal-Fetal Interface

To determine the cell-type localization of TAP2 in the endometrium, we used data from the Human Protein Atlas immunohistochemistry collection[24] for the endometrium, placenta, and decidua. Using previously generated microarray expression data, we examined the expression of *TAP2* in the endometrium across the menstrual cycle,[25] in mid-secretory-phase endometrial biopsies from women not taking hormonal contraceptives (n = 11), in women using either of the progestin-based contraceptives depot medroxyprogesterone acetate (DMPA) and levonorgestrel intrauterine system (LNG-IUS) for at least 6 months,[26] and in DSCs treated with a progesterone receptor (PGR)-specific small interfering RNA (siRNA) or a non-targeted siRNA.[27] These microarray datasets were analyzed with the GEO2R analysis package, which implements the GEOquery[28] and limma R packages[29,30] from the Bioconductor project to quantify differential gene expression. We also examined *TAP2* expression in RNA-sequencing (RNA-seq) data previously generated from ESFs treated with control media or differentiated (decidualized) with cAMP and medroxyprogesterone acetate (MPA) into DSCs.[31,32]

rs2071473 Is Located within a cAMP- and Progesterone-Responsive Regulatory Element and Disrupts Putative DDIT3 Binding

A 1,000 bp region spanning 50 bp upstream of rs2071473 to the 3′ end of the PGR chromatin immunoprecipitation sequencing (ChIP-seq) peak was cloned into the pGL3-Basic luciferase vector (Promega) once with the T allele and once with the C allele (GenScript). A pGL3-Basic plasmid without the 1 kb rs2071473 insert was used as a negative control. DDIT3 and PGR expression vectors were also obtained from GenScript. ESFs (ATCC CRL-4003) immortalized with telomerase were maintained in phenol-red-free DMEM (GIBCO) supplemented with 10% charcoal-stripped fetal bovine serum (CSFBS, GIBCO), 1× insulin-transferrin-selenium (GIBCO), 1% sodium pyruvate (GIBCO), and 1% L-glutamine (GIBCO). Confluent ESFs in 96-well plates in 80 μL of Opti-MEM (GIBCO) were transfected with 100 ng of the luciferase plasmid, 100 ng of DDIT3 and/or PGR as needed, and 10 ng of pRL-null with 0.1 μL of PLUS reagent (Invitrogen) and 0.25 μL of Lipofectamine LTX (Invitrogen) in 20 μL of Opti-MEM. The cells were incubated in the transfection mixture for 6 hr, and the media were replaced with the phenol-red-free maintenance media overnight. Then, for inducing decidualization, cells were incubated in the decidualization media (DMEM with phenol red [GIBCO], 2% CSFBS [GIBCO], 1% sodium pyruvate [GIBCO], 0.5 mM 8-Br-cAMP [Sigma], and 1 μM medroxyprogesterone acetate [Sigma]) for 48 hr. Decidualization controls were incubated in the decidualization control media (phenol-red-free DMEM [GIBCO], 2% CSFBS [GIBCO], and 1% sodium pyruvate [GIBCO]) instead for 48 hr. After decidualization, Dual Luciferase Reporter Assays (Promega) began with incubating the cells for 15 min in 20 μL of 1× passive lysis buffer. Luciferase and *Renilla* activity was then measured with the Glomax multi+ detection system (Promega). We standardized luciferase activity values to *Renilla* activity values and background activity values by measuring luminescence from the pGL3-Basic plasmid with no insert.

The rs2071473 C Allele Is Derived in Humans and Segregates at Intermediate to High Frequencies across Multiple Human Populations

To reconstruct the evolutionary history of the T/C polymorphism, we used a region spanning 50 bp upstream and downstream of rs2071473 from UCSC Genome Browser build hg19 (chr6: 32814778–32814878) as a query sequence to BLAT search the chimpanzee (CHIMP2.1.4), gorilla (gorGor3.1), organutan (PPYG2), gibbon (Nleu1.0), rhesus monkey (MMUL_1), hamadryas baboon (Pham_1.0), olive baboon (Panu_2.0), vervet monkey (ChlSab1.0), marmoset (C_jacchus3.2.1), Bolivian squirrel monkey (SalBol1.0), tarsier (tarSyr1), mouse lemur (micMur1), and galago (OtoGar3) genomes. For all other non-human species, we used the same 101 bp region as a query for Sequence Read Archive (SRA) Nucleotide BLAST against high-throughput sequencing reads deposited in the SRA. The 100 top-scoring reads were assembled into contigs with the "Map to reference" option in Geneious v.6.1.2 and the human sequence as a reference. Sequences for the Altai Neanderthal, Denisovan, Ust'-Ishim, and two aboriginal Australians were obtained from the Ancient Genome Browser of the Max Planck Institute for Evolutionary Anthropology. The frequency of the T/C allele across the Human Genome Diversity Project (HGDP) populations was obtained from the Geography of Genetic Variants Browser of the University of Chicago.

We inferred ancestral sequences of the 101 bp region by using the Ancestral Sequence Reconstruction (ASR) module of Datamonkey[33] (which implements joint, marginal, and sampled reconstruction methods),[34] the nucleotide alignment of the 101 bp region, the best-fitting nucleotide-substitution model (HKY85), a general discrete model of site-to-site rate variation with three rate classes, and the phylogeny shown in Figure 4A. All three ASR methods reconstructed the same sequence for the ancestral human sequence at 1.0 support.

rs2071473 Has Signatures of Balancing Selection in Humans and Diversifying Selection in Primates

To infer whether there is evidence of positive selection acting on the derived T allele, we used an improved version of the EvoNC method[35] that has been modified into a branch-site model[36,37] and implemented in HyPhy v2.22.[37,38] This method utilizes the MG94HKY85 nucleotide-substitution model, which was also the best-fitting nucleotide-substitution model for our target non-coding region and neutral rate proxy, and includes ten replicate likelihood searches. Although this implementation of the EvoNC method has been modified into a branch-site model capable of identifying positively selected sites in a priori defined lineages via naive empirical Bayes (NEB) and Bayes empirical Bayes (BEB) approaches, previous studies have shown that these methods have high type I and type II error rates. Therefore, we inferred evidence without reference to NEB- or BEB-identified sites and instead relied on a significant likelihood-ratio test (LRT) between the null and alternative models. We analyzed an alignment of

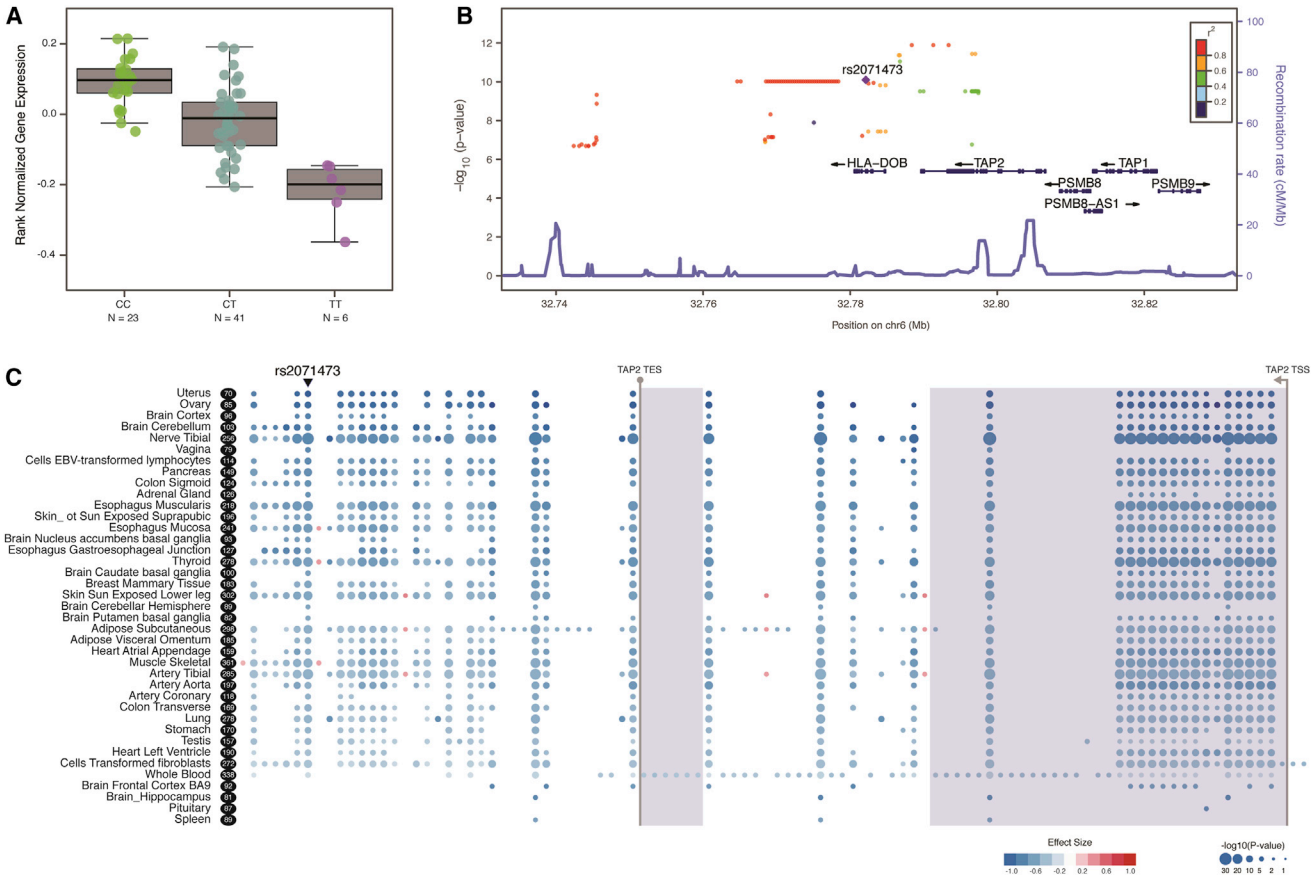

Figure 1. Replication of the rs2071473 T/C Polymorphism as an eQTL for *TAP2*
(A) Boxplots of uterine *TAP2* expression from GTEx data. Below each boxplot is the number of individuals with each genotype.
(B) Region association plot showing GTEx SNPs that are significant eQTLs for *TAP2* expression ($-\log_{10}$ p value, left y axis). SNPs are color coded on the basis of their LD with rs2071473 (purple diamond). Local recombination rates are shown on the right y axis.
(C) Gene-eQTL visualizer plot showing significant eQTLs for *TAP2* (see inset key for $-\log_{10}$ p value and effect-size coding) across 39 GTEx tissues. Tissues are sorted by largest effect size from top to bottom. Numbers in black ovals indicate sample sizes. The locations of *TAP2* coding exons are shown with light-blue shading, and the transcription start site (TSS) and transcription end site (TES) are indicated.

the 101 bp region described above, the phylogeny shown in Figure 4A, and synonymous sites from the flanking genes *HLA-DOB* and *TAP2*, which were identified from the same primate species by the method described above. F_{ST}, Tajima's D, and Fay and Wu's H data for CEU (Utah residents [CEPH] with northern and western European ancestry) and YRI (Yoruba in Ibadan, Nigeria) populations were obtained from the 1000 Genomes Selection Browser 1.0.[39]

Results

rs2071473 Is a Multi-tissue eQTL for *TAP2*, *HLA-DOB*, and *HLA-DRB6*

We have previously shown that a T/C polymorphism at rs2071473 is an eQTL for *TAP2* in mid-secretory-phase endometrium.[15] To replicate this observation in an independent cohort and in additional tissues, we used GTEx data to test whether rs2071473 is correlated with *TAP2* expression. Similarly to our previous observation, we found that rs2071473 is an eQTL for *TAP2* in GTEx uterus samples ($n = 70$, $\beta = -1.1$, $p = 9.1 \times 10^{-11}$; Figures 1A and 1B) as well as 34 other tissues (Figure 1C); the largest effect size was observed in the uterus (Figure 1C). We also used GTEx data to identify other genes for which rs2071473 is an eQTL and found that it is an eQTL for *HLA-DOB* in 25 tissues ($\beta = -0.27$ to -0.91, $p = 5.4 \times 10^{-9}$–9.1×10^{-20}; Table S1) and for *HLA-DRB6* in four tissues ($\beta = 0.37$–0.46, $p = 6.7 \times 10^{-6}$–2.1×10^{-8}; Table S1). However, rs2071473 was not identified as a uterine eQTL for *HLA-DOB* or *HLA-DRB6* because neither gene is expressed in GTEx uterine tissues.

TAP2 Is Expressed by DSCs at the Maternal-Fetal Interface

Although *TAP2* is expressed in uterine tissues, the mid-secretory-phase endometrium is a complex tissue composed of numerous cell types, including perivascular mesenchymal stem-like cells,[19,40] ESFs,[18] DSCs,[17,18] luminal and glandular epithelial cells, endothelial cells lining blood vessels, uterine natural killer (uNK) cells,[41] uterine macrophages (uMPs),[42,43] multiple populations of T cells,[44–47] and dendritic cells,[48,49] among many others. To determine which cell types produce TAP2, we examined

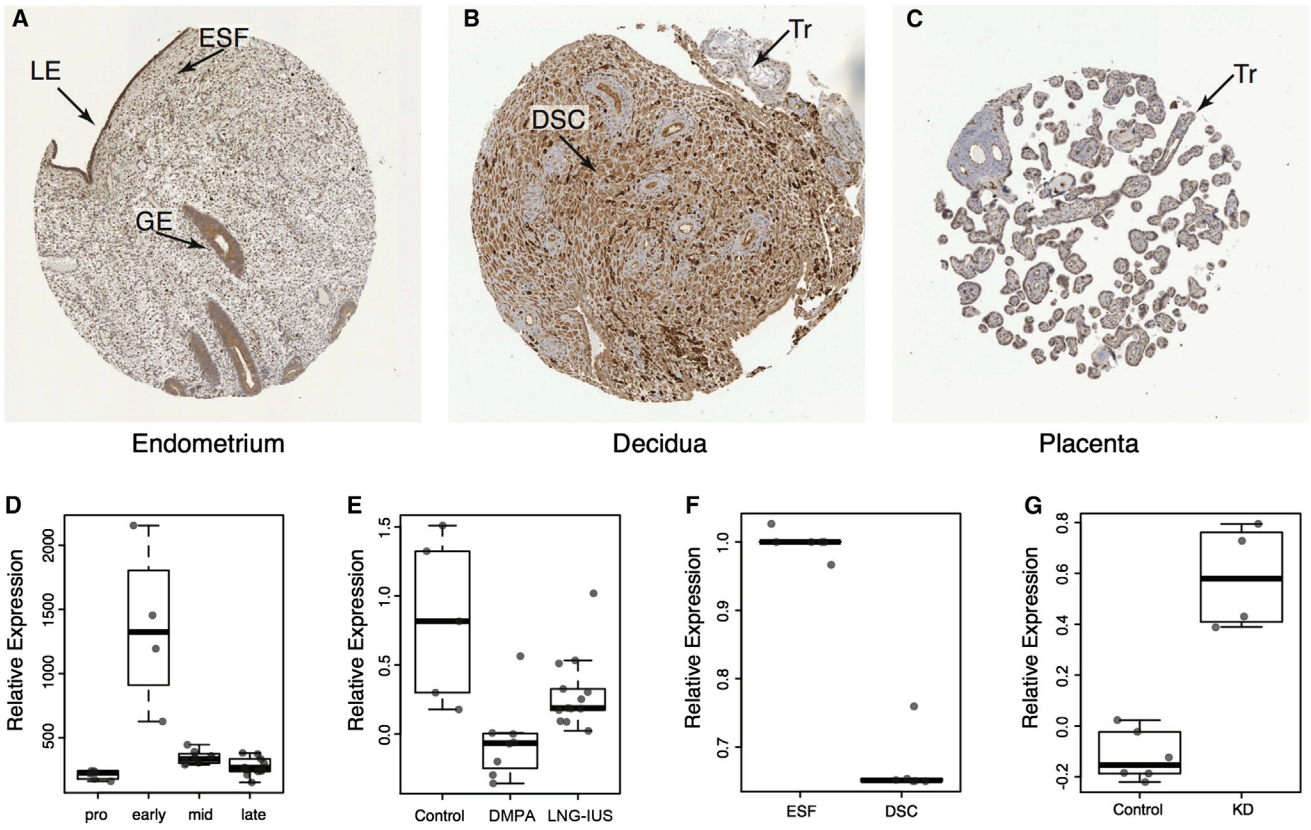

Figure 2. *TAP2* Is Regulated by Progesterone and Is Expressed by DSCs at the Maternal-Fetal Interface
(A–C) Immunohistochemistry staining showing TAP2 localization in the (A) non-pregnant endometrium, (B) pregnant endometrium (decidua), and (C) placenta. Abbreviations are as follows: LE, luminal epithelium; GE, glandular epithelium; ESF, endometrial stromal fibroblast; DSC, decidual stromal cell; and Tr, trophoblast.
(D) Relative expression of *TAP2* across the menstrual cycle.
(E) Relative expression of *TAP2* in the endometrium of women using either depot medroxyprogesterone acetate (DMPA) or levonorgestrel intrauterine system (LNG-IUS), both progestin-based contraceptives.
(F) Relative expression of *TAP2* in ESFs treated with control media or differentiated into DSCs with cAMP and MPA for 48 hr.
(G) Relative expression of *TAP2* in cAMP- and MPA-differentiated DSCs treated with a control siRNA or a PGR-specific siRNA (KD).

its localization in endometrial biopsies from the Human Protein Atlas immunohistochemistry collection. We found that TAP2 staining was localized primarily to the luminal and glandular epithelium and ESFs in non-pregnant endometrium (Figure 2A), was particularly intense in DSCs in pregnant endometrium (Figure 2B), and was absent from trophoblast cells (Figures 2B and 2C). Thus, TAP2 is produced by maternal cells, particularly DSCs, at the maternal-fetal interface.

Next, we tracked the expression of *TAP2* in the endometrium across the menstrual cycle by using previously generated microarray expression data.[25] We found that *TAP2* expression reached its peak during the early secretory phase of the menstrual cycle and rapidly decreased in the mid-secretory phase (Figure 2D), suggesting that downregulation of *TAP2* is regulated by progesterone and associated with endometrial receptivity to implantation. To infer whether *TAP2* expression in the endometrium is regulated by progesterone, we took advantage of an existing gene-expression dataset of mid-secretory-phase endometrial biopsies from women not taking hormonal contraceptives ($n = 11$) and women using either of the progestin-based contraceptives DMPA and LNG-IUS for at least 6 months.[26] Consistent with regulation by progesterone, we found that *TAP2* expression was significantly lower in the endometria of women taking DMPA ($p = 0.002$) or LNG-IUS ($p = 0.012$) than in control women (Figure 2E).

To directly test whether *TAP2* is regulated by progesterone, we examined its expression in RNA-seq data from ESFs treated with control media or differentiated (decidualized) with cAMP and MPA into DSCs[31,32] and found that *TAP2* was downregulated ~33% by cAMP and MPA treatment (Figure 2F). To test whether these effects were mediated by PGR, we used a previously published dataset to compare *TAP2* expression in DSCs treated with a PGR-specific siRNA or a non-targeted siRNA[27] and found that knockdown of PGR significantly upregulated *TAP2* expression in DSCs ($p = 0.01$; Figure 2G). Thus, we conclude that *TAP2* is downregulated by progesterone during the differentiation of ESFs into DSCs and in the endometrium during the period of endometrial receptivity to implantation.

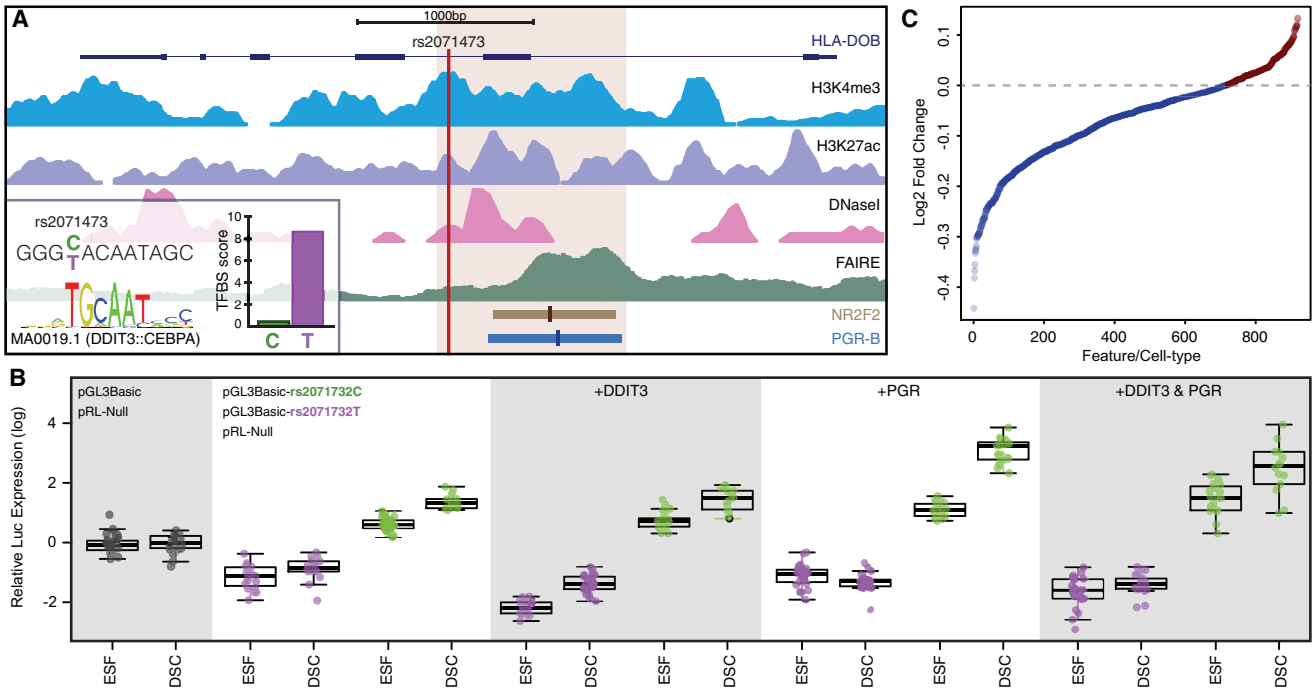

Figure 3. The T/C Polymorphism at rs2071473 Is Located within a Progesterone-Responsive *cis*-Regulatory Element in DSCs

(A) Location of rs2071473 with respect to histone modifications that characterize promoters (H3K4me4 ChIP-seq), enhancers (H3K27ac ChIP-seq), open chromatin (DNaseI-seq and FAIRE-seq), and PGR and NR2F2 ChIP-seq binding sites. Inset: the rs2071473 C allele is predicted to disrupt a DDIT3 binding site. The 1 kb region shown in light brown was cloned into the pGL3Basic luciferase reporter vector for functional characterization.

(B) Results of the luciferase assay testing the regulatory potential of the T (pGL3Basic-rs2071473T) and C (pGL3Basic-rs2071473C) alleles in ESFs treated with control media or differentiated into DSCs with cAMP and MPA for 48 hr. Data are shown as luciferase activity from the pGL3Basic-rs2071473C or pGL3Basic-rs2071473T reporter in relation to *Renilla* activity (pRL-null and empty vector [pGL3Basic] controls). Abbreviations are as follows: +DDIT3, relative luciferase activity from pGL3Basic-rs2071473C or pGL3Basic-rs2071473T in ESFs and DSCs co-transfected with DDIT3; +PGR, relative luciferase activity from pGL3Basic-rs2071473C or pGL3Basic-rs2071473T in ESFs and DSCs co-transfected with PGR; and +DDIT3 & PGR, relative luciferase activity from pGL3Basic-rs2071473C or pGL3Basic-rs2071473T in ESFs and DSCs co-transfected with DDIT3 and PGR.

(C) DeepSea-predicted effects ($\log_2$ fold change) of rs2071473 on regulatory features across cell types.

The rs2071473 Variant Switches a Repressor into an Activator

Our observations that rs2071473 is an eQTL for *TAP2* and that *TAP2* expression is downregulated by progesterone suggests that rs2071473 might be located within or linked to a progesterone-responsive enhancer. To identify such a regulatory element, we used previously obtained ChIP-seq data from DSCs for the transcription factors PGR[32,50,51] and NR2F2 (COUP-TFII)[52] (which regulate the transcriptional response to progesterone and immune genes, respectively), H3K27ac (which marks active enhancers), and H3K4me3 (which marks active promoters),[32] as well as DNaseI-seq and FAIRE-seq data, to identify regions of open chromatin.[32] We found that rs2071473 was located 260 bp upstream of PGR and NR2F2 binding sites, within local DNaseI and FAIRE peaks, and in a region of elevated H3K4me3 and H3K27ac signal (Figure 3A), suggesting that this region is a progesterone-responsive *cis*-regulatory element.

To test whether this locus has regulatory potential, we synthesized a 1,000 bp region spanning 50 bp upstream of rs2071473 to the 3′ end of the PGR ChIP-seq peak (Figure 3A) with either the reference C allele or the alternative T allele and cloned them into the pGL3-Basic luciferase reporter vector, which lacks both an endogenous promoter and an enhancer. Next, we transiently transfected either the pGL3Basic-rs2071473T or pGL3Basic-rs2071473C luciferase reporter along with the pRL-null internal control vector into ESFs and DSCs and quantified luciferase and *Renilla* activity by using a dual luciferase assay.

We found that luciferase activity was significantly lower in ESFs (Wilcox test $p = 1.75 \times 10^{-11}$) and DSCs (Wilcox test $p = 2.87 \times 10^{-9}$) transfected with the pGL3Basic-rs2071473T reporter than in pGL3Basic empty-vector controls (Figure 3B). In stark contrast, luciferase activity was significantly higher in ESFs (Wilcox test $p = 1.42 \times 10^{-9}$) and DSCs (Wilcox test $p = 2.53 \times 10^{-13}$) transfected with the pGL3Basic-rs2071473C reporter than in controls (Figure 3B). The difference in luciferase activity between pGL3Basic-rs2071473T and pGL3Basic-rs2071473C was also significant in ESFs (Wilcox test $p = 2.50 \times 10^{-12}$) and DSCs (Wilcox test $p = 1.76 \times 10^{-11}$). Luciferase activity was significantly induced upon differentiation

of ESFs to DSCs by cAMP and MPA treatment in both pGL3Basic-rs2071473T-transfected cells (Wilcox test $p = 0.02$) and pGL3Basic-rs2071473C-transfected cells (Wilcox test $p = 2.53 \times 10^{-13}$) (Figure 3B). Thus, we conclude that the locus in which rs2071473 resides is a progesterone-responsive *cis*-regulatory element and that the T/C polymorphism switches an enhancer into a repressor.

The rs2071473 C Allele Most Likely Disrupts a DDIT3 Binding Site

The T/C polymorphism at rs2071473 is several hundred base pairs away from the PGR and NR2F2 binding sites and is therefore unlikely to directly affect their binding (Figure 3A). However, our luciferase assay results indicate that the T/C polymorphism has regulatory effects, suggesting that this polymorphism disrupts a binding site for a transcriptional repressor or creates a binding site for a transcriptional activator. To infer which of these scenarios is most likely, we identified putative transcription factor binding sites in a 25 bp window upstream and downstream of rs2071473 by using ConSite[53] and JASPAR transcription factor binding site profiles.[54] We found that the T/C polymorphism occurs at an invariant T site in the DDIT3 motif (TGCAAT) and is predicted to abolish DDIT3 binding (Figure 3A, inset). Similarly, the T/C polymorphism was predicted by DeepSea[55] (a deep-learning-based algorithm that infers the effects of single-nucleotide substitutions on chromatin features such as transcription factor binding, DNase I sensitivity, and histone marks) to generally have a negative effect on regulatory functions across multiple cell types (Figure 3C).

Although DDIT3 (also known as CHOP10 and GADD153) was initially characterized as a dominant-negative inhibitor of CEBP family transcription factors,[56] it can also function as a transcription factor[57,58] and is transcriptionally regulated by cAMP.[59] Indeed, we found that *CHOP10* expression was downregulated by cAMP and MPA in our RNA-seq data from ESFs (transcripts per million [TPM] = 187.68) and DSCs (TPM = 61.20). These data suggest that the T/C polymorphism might disrupt a DDIT3 binding site that mediates transcriptional repression of *TAP2*, unmasking a secondary enhancer function. To test this hypothesis, we co-transfected ESFs and DSCs with a DDIT3 expression vector, the pRL-null internal control vector, and either the pGL3Basic-rs2071473T or thepGL3Basic-rs2071473C luciferase reporter and compared luciferase activity to that of control ESFs and DSCs. If DDIT3 mediates repression by binding the T allele, then co-transfection of DDIT3 with the pGL3Basic-rs2071473T reporter should augment repression, whereas co-transfection with the pGL3Basic-rs2071473C reporter should be unaffected. Indeed, the addition of DDIT3 significantly reduced luciferase activity from the pGL3Basic-rs2071473T reporter in ESFs (Wilcox test $p = 3.48 \times 10^{-10}$) and DSCs (Wilcox test $p = 1.591 \times 10^{-5}$) but had no effect on luciferase activity from the pGL3Basic-rs2071473C reporter in either ESFs or DSCs ($p > 0.21$; Figure 3B).

To test whether this regulatory element is responsive to progesterone, we co-transfected ESFs and DSCs with a PGR rather than a DDIT3 expression vector and repeated the luciferase assays described above. The addition of PGR did not affect luciferase activity from the pGL3Basic-rs2071473T reporter in ESFs (Wilcox test $p = 0.67$) but did enhance repression in DSCs (Wilcox test $p = 9.56 \times 10^{-5}$; Figure 3B). Co-transfection of PGR elevated luciferase activity from the pGL3Basic-rs2071473C reporter in both ESFs (Wilcox test $p = 2.82 \times 10^{-8}$) and DSCs (Wilcox test $p = 2.53 \times 10^{-13}$; Figure 3B). Finally, we tested whether DDIT3 and PGR act co-operatively or antagonistically by co-transfecting both the DDIT3 and PGR expression vectors with either the pGL3Basic-rs2071473T or the pGL3Basic-rs2071473C reporter into ESFs and DSCs. Consistent with a weakly antagonistic functional interaction, luciferase activity in ESFs and DSCs transfected with both DDIT3 and PGR fell between the activity in DDIT3-tranfected cells and the activity in PGR-transfected cells (Figure 3B). These data suggest that the reference C allele most likely disrupts a DDIT3 biding site, which unmasks a progesterone-responsive enhancer.

The rs2071473 C Allele Is Derived in Humans and Has Evidence of Positive Selection

To reconstruct the evolutionary history of the T/C polymorphism, we identified a region spanning 50 bp upstream and downstream of rs2071473 from 45 primates, including species from each of the major primate lineages, multiple sub-species of African apes (Homininae), and modern and archaic (Altai Neanderthal and Denisovan) humans. Next, we used maximum-likelihood methods to reconstruct ancestral sequences for this 101 bp region. We found that the T allele was ancestral in primates and that the C variant was found in only modern human populations and the Altai Neanderthal genome (Figure 4A). Next, we examined the frequency of these alleles across the HGDP populations as well as two aboriginal Australians and found that the derived and ancestral alleles segregated at intermediate to high frequencies in nearly all human populations (Figure 4B). These results indicate that the derived C variant at rs2071473 arose before the divergence of modern and archaic human lineages.

To test whether the derived C allele might have been positively selected, we used a branch-site version of the EvoNC method.[35–37] In this analysis, the nucleotide-substitution rate in non-coding regions (d_{nc}) is compared with a neutral rate proxy from either introns or synonymous substitutions (d_S) in nearby coding genes. The strength and direction of selection acting on non-coding regions is given by d_{nc}/d_S (or ζ), which is analogous to the d_N/d_S rate (or ω), where $\zeta = 1$ indicates neutral evolution, $\zeta < 1$ indicates negative (purifying) selection, and $\zeta > 1$ indicates positive selection. We analyzed the 101 bp region described above and synonymous sites from the flanking genes *HLA-DOB* and *TAP2* and fit three models to the data: (1) a null model that constrains

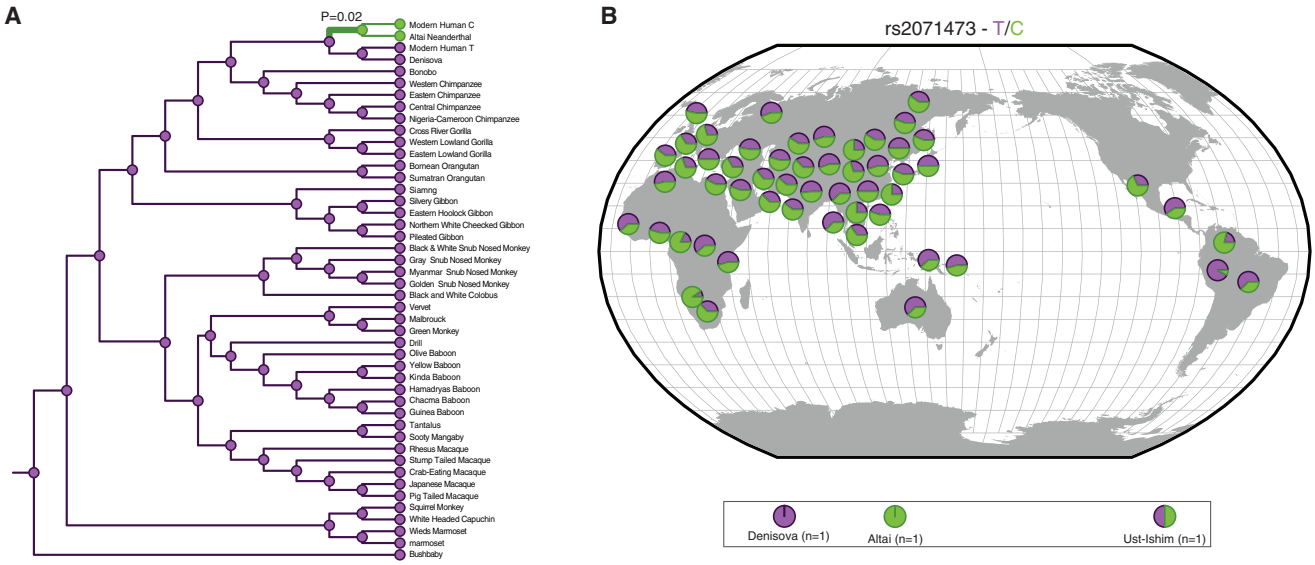

Figure 4. Evolutionary History of the T/C Polymorphism at rs2071473
(A) rs2071473 genotype across extant and ancestral primates. Genotypes in extant species are shown as circles next to species names at terminal branches. Genotypes at internal nodes based on ancestral reconstruction are shown as circles. The T allele is shown in purple, and the C allele is shown in green. p = 0.02 indicates that the lineage was identified as positively selected by the branch-site version of the EvoNC method.
(B) Distribution of the T and C alleles of rs2071473 across HGDP populations.

$\zeta \leq 1$ across all sites and lineages, (2) an alternative model that allows for $\zeta \leq 1$ in foreground and background branches, $\zeta \leq 1$ in background branches, and $\zeta > 1$ in the foreground branch, and (3) an alternative model that allows for $\zeta < 1$ in foreground and background branches, $\zeta = 1$ in foreground and background branches, $\zeta < 1$ in background and $\zeta > 1$ in foreground branches, and $\zeta = 1$ in background and $\zeta > 1$ in foreground branches. The null model was rejected in favor of both alternative model 1 (LRT = 5.37, p = 0.02) and alternative model 2 (LRT = 5.38, p = 0.02), suggesting that the T>C substitution might have been positively selected.

rs2071473 Has Signatures of Balancing Selection in Humans and Diversifying Selection in Primates

Our observation that the C allele originated before the divergence of modern and archaic humans and segregates at intermediate frequencies across modern human populations suggests that the ancestral and derived variants could be maintained by balancing selection. Previous studies have shown that balancing selection is common in the HLA region in which *TAP2* and rs2071473 are located.[60–63] DeGiorgio et al., for example, developed a model-based approach to identify signatures of ancient balancing selection and found that the *HLA-DOB* locus, which includes rs2071473, was an outlier (top 0.5% of all scores across the genome) in their scan for balancing selection.[64] Consistent with the action of long-term balancing selection, rs2071473 has essentially no differentiation between populations (F_{ST} = 0–0.016) and is located in a region with a relative excess of common polymorphisms across CEU and YRI populations, as measured by Tajima's D (1.16–2.07), Fay and Wu's H (−23.16 to −56.83), and pi (86.41–107.71) (Figure 5).

To test whether the rs2071473 enhancer region evolved under positive diversifying selection across primates, we used the site version of the EvoNC method.[35–37] We fit three models to the alignment described above: (1) a null model that constrains $\zeta \leq 1$ across all sites, (2) an alternative model that allows for categories of sites with $\zeta \geq 1$ and $\zeta < 1$, and (3) an alternative model that allows for categories of sites with $\zeta < 1$, $\zeta = 1$, or $\zeta > 1$. We found that the null model was not rejected in favor of alternative model 1 (LRT = 0, p = 1); however, alternative model 2 was a better fit to the data than either the null model (LRT = 11.76, p = 0.019) or alternative model 1 (LRT = 11.78, p = 0.0005). These data indicate that including distinct rate classes for sites with $\zeta < 1$ or $\zeta = 1$ significantly improves the alternative model and suggest that positive diversifying selection acts on sites in this regulatory element across primates.

Discussion

The mechanisms that promote maternal tolerance of the antigenically distinct fetus are complex[65] and have been the subject of intense study since Medawar formulated the immunological paradox posed by pregnancy and proposed that tolerance is achieved by physical separation of maternal and fetal tissues, maternal immunosuppression, and immaturity of fetal antigens.[66] It is now clear that rather than being a site of maternal immunosuppression,[67] the maternal immune system in the endometrium

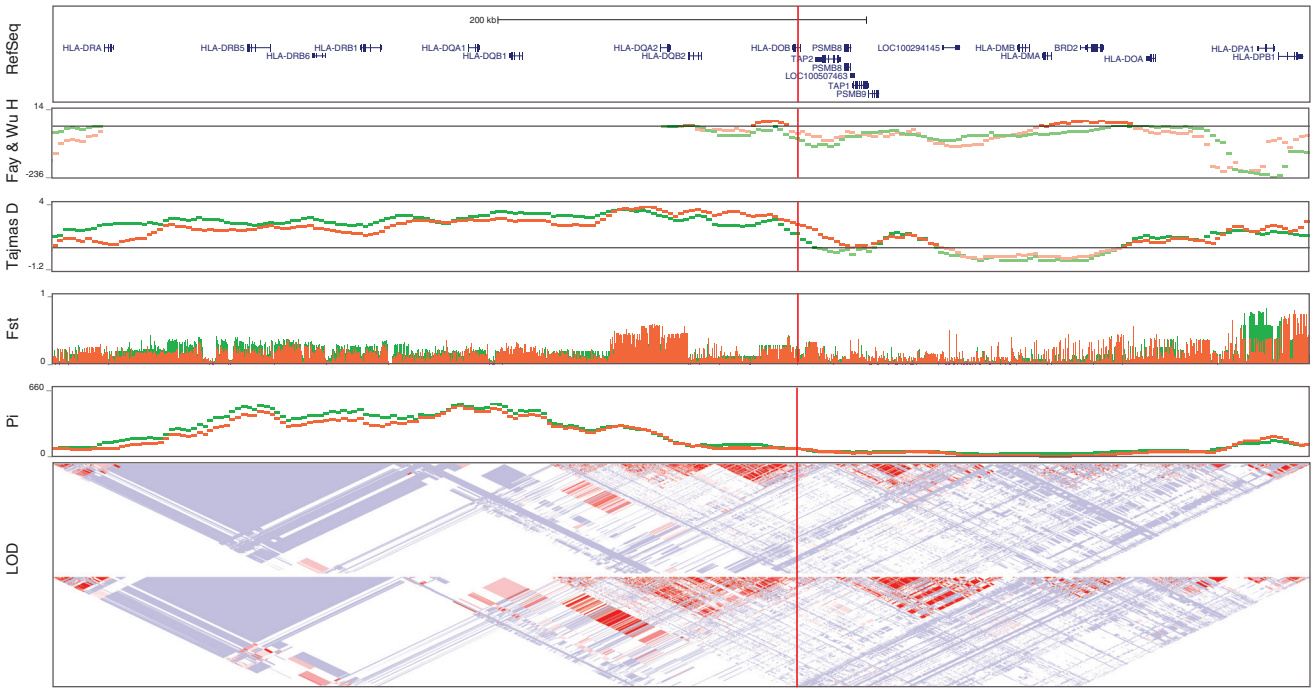

Figure 5. The rs2071473 T/C Polymorphism Has Genetic Signatures of Balancing Selection
Fay and Wu's H statistic, Tajima's D, F_{ST}, and nucleotide diversity (pi) for HGDP CEU (green) and YRI (red) populations across the HLA region of chromosome 6. The location of rs2071473 is shown with a vertical red line. LD across this region is shown, LOD scores with white diamonds indicate pairwise D′ values less than 1 with no statistically significant evidence of LD (LOD < 2), light-blue diamonds indicate high D′ values (>0.99) with low statistical significance (LOD < 2), and light-pink diamonds indicate high statistical significance (LOD ≥ 2) but low D′ (<0.5).

plays an active role in establishing a permissive environment for implantation, placentation, and gestation. For example, maternal regulatory T cells,[45,68] shifts in the Th1-Th2-Th17 cell balance,[46] uNK cells,[41,69] uterine dendritic cells,[48] uMPs,[70] and signaling by DSCs[71–73] all contribute to establishing immunotolerance and even promote placental invasion into maternal tissues.

It has also become clear that the MHC genes, which play an important role in the rejection of non-self-tissues, contribute to maternal tolerance of the fetus.[21] HLA antigen matches between couples, for example, are associated with longer intervals from marriage to birth than are HLA antigen mismatches between couples;[74,75] these longer intervals result from both higher miscarriage rates among couples with matching class I HLA-B antigens[14] and longer intervals to pregnancy among couples with matching class II HLA-DR antigens.[13] Similarly, the non-classical HLA class I gene *HLA-F* (MIM: 143110) is associated with fecundability, whereas overwhelming evidence indicates that maternal and fetal HLA-G genotypes are associated with miscarriage, recurrent pregnancy loss, and preeclampsia.[76–87] Collectively, these data implicate antigen presentation by the MHC as one of the molecular mechanisms that underlie successful implantation, maternal immunotolerance, and the establishment and maintenance of pregnancy.

The ATP-binding cassette transporter TAP, a heterodimer composed of TAP1 and TAP2, translocates peptides from the cytosol to awaiting MHC class I molecules in the endoplasmic reticulum, which results in cell-surface presentation of the trimeric MHC complex to immune cells such as T lymphocytes and natural killer cells.[20] Lost and reduced TAP accumulation leads to lost and reduced surface HLA accumulation,[88–90] altered surface HLA repertoires,[91] and the surface presentation of distinct antigenic peptides that are recognized by cytotoxic T lymphocytes.[92] Our observation that *TAP2* is highly expressed by DSCs at the maternal-fetal interface and that *TAP2* expression levels are associated with fecundability suggests that changes in TAP2 stoichiometry could alter MHC processing and thus interactions between DSCs and maternal immune cells. Indeed, DSCs produce numerous HLA class I molecules, including HLA-G and HLA-F[93] (C. Reyes-Perdomo et al., 2013, Int. Congr. Immun., conference), which are transcriptionally upregulated by progesterone during decidualization.[73]

Although the connection between TAP2 levels in DSCs and immune signaling are obvious, our observation that the ancestral and derived alleles of rs2071473 arose before the divergence of modern and archaic humans and have signatures of long-term balancing selection is unexpected. The HLA region has long been recognized to be under balancing selection.[60,61,64,94,95] These signals, however, are usually attributed to polymorphisms within the classical HLA class I genes rather than regulatory regions.[96] *TAP2* and rs2071473 are also located near the distal end

of the HLA region and bounded by regions of high recombination, including a recombination hotspot within *TAP2*,[97] and in a linkage disequilibrium (LD) block that includes few other HLA genes. These data suggest that the signal of balancing selection at rs2071473 is distinct from other signals of balancing selection in the HLA region, but it is difficult to disentangle these signals given the relatively strong linkage across the HLA region. Thus, it is possible that the T/C polymorphism at rs2071473 is not itself under balancing selection and is linked to the balanced site.

If the target of balancing selection is rs2071473, what selective forces are acting to maintain the ancestral and derived alleles? Balancing selection is generally attributed to heterozygote advantage (overdominance), frequency-dependent selection, or antagonistic pleiotropy,[98] which are all probable evolutionary scenarios to explain maintenance of the ancestral and derived alleles of rs2071473. Intriguingly, GWASs have found that the rs2071473 genotype is associated with ulcerative colitis (MIM: 266600),[99] Crohn disease (MIM: 266600),[100] and sarcoidosis (MIM: 609464),[101,102] in addition to fecundability. For example, the ancestral T allele is significantly associated with ulcerative colitis[99] and shorter time to pregnancy, whereas the derived C allele is significantly associated with Crohn disease[100] and longer time to pregnancy, suggesting that these alleles could be maintained by antagonistic pleiotropy. These data are strong examples of a reproduction-health tradeoff in human evolution.

Supplemental Data

Supplemental Data include one table and can be found with this article online at http://dx.doi.org/10.1016/j.ajhg.2016.09.002.

Acknowledgments

This work was funded by a Burroughs Wellcome Fund Preterm Birth Initiative grant (1013760), an NIH National Institute of General Medical Sciences graduate training grant (T32GM007197), and the March of Dimes Prematurity Research Center at the University of Chicago, Northwestern, and Duke. The authors thank C. Ober for comments on an earlier version of this manuscript.

Received: June 27, 2016
Accepted: September 2, 2016
Published: October 13, 2016

Web Resources

1000 Genomes Selection Browser 1.0, http://hsb.upf.edu
Adaptive Evolution Server at Datamonkey.org, http://www.datamonkey.org
Ancient Genome Browser, http://www.eva.mpg.de/neandertal/index.html
GEO2R, http://www.ncbi.nlm.nih.gov/geo/geo2r/
Geography of Genetic Variants Browser, http://popgen.uchicago.edu/ggv/
GTEx Portal, http://www.gtexportal.org/home/eqtls/bySnp
OMIM, http://www.omim.org
The Human Protein Atlas immunohistochemistry collection, http://www.proteinatlas.org/
UCSC Genome Browser, http://genome.ucsc.edu

References

1. Kosova, G., Abney, M., and Ober, C. (2010). Colloquium papers: Heritability of reproductive fitness traits in a human population. Proc. Natl. Acad. Sci. USA *107* (*Suppl 1*), 1772–1778.
2. Christensen, K., Kohler, H.P., Basso, O., Olsen, J., Vaupel, J.W., and Rodgers, J.L. (2003). The correlation of fecundability among twins: evidence of a genetic effect on fertility? Epidemiology *14*, 60–64.
3. Tropf, F.C., Verweij, R.M., van der Most, P.J., and Stulp, G. (2016). Mega-analysis of 31,396 individuals from 6 countries uncovers strong gene-environment interaction for human fertility. bioRxiv, http://dx.doi.org/10.1101/049163.
4. Ruth, K.S., Beaumont, R.N., Tyrrell, J., Jones, S.E., Tuke, M.A., Yaghootkar, H., Wood, A.R., Freathy, R.M., Weedon, M.N., Frayling, T.M., and Murray, A. (2016). Genetic evidence that lower circulating FSH levels lengthen menstrual cycle, increase age at menopause and impact female reproductive health. Hum. Reprod. *31*, 473–481.
5. Elks, C.E., Perry, J.R., Sulem, P., Chasman, D.I., Franceschini, N., He, C., Lunetta, K.L., Visser, J.A., Byrne, E.M., Cousminer, D.L., et al.; GIANT Consortium (2010). Thirty new loci for age at menarche identified by a meta-analysis of genome-wide association studies. Nat. Genet. *42*, 1077–1085.
6. He, C., Kraft, P., Chen, C., Buring, J.E., Paré, G., Hankinson, S.E., Chanock, S.J., Ridker, P.M., Hunter, D.J., and Chasman, D.I. (2009). Genome-wide association studies identify loci associated with age at menarche and age at natural menopause. Nat. Genet. *41*, 724–728.
7. Perry, J.R.B., Day, F., Elks, C.E., Sulem, P., Thompson, D.J., Ferreira, T., He, C., Chasman, D.I., Esko, T., Thorleifsson, G., et al.; Australian Ovarian Cancer Study; GENICA Network; kConFab; LifeLines Cohort Study; InterAct Consortium; Early Growth Genetics (EGG) Consortium (2014). Parent-of-origin-specific allelic associations among 106 genomic loci for age at menarche. Nature *514*, 92–97.
8. Stolk, L., Perry, J.R.B., Chasman, D.I., He, C., Mangino, M., Sulem, P., Barbalic, M., Broer, L., Byrne, E.M., Ernst, F., et al.; LifeLines Cohort Study (2012). Meta-analyses identify 13 loci associated with age at menopause and highlight DNA repair and immune pathways. Nat. Genet. *44*, 260–268.
9. Chen, C.T.L., Liu, C.-T., Chen, G.K., Andrews, J.S., Arnold, A.M., Dreyfus, J., Franceschini, N., Garcia, M.E., Kerr, K.F., Li, G., et al. (2014). Meta-analysis of loci associated with age at natural menopause in African-American women. Hum. Mol. Genet. *23*, 3327–3342.
10. Mbarek, H., Steinberg, S., Nyholt, D.R., Gordon, S.D., Miller, M.B., McRae, A.F., Hottenga, J.J., Day, F.R., Willemsen, G., de Geus, E.J., et al. (2016). Identification of Common Genetic Variants Influencing Spontaneous Dizygotic Twinning and Female Fertility. Am. J. Hum. Genet. *98*, 898–908.
11. Aschebrook-Kilfoy, B., Argos, M., Pierce, B.L., Tong, L., Jasmine, F., Roy, S., Parvez, F., Ahmed, A., Islam, T., Kibriya,

M.G., and Ahsan, H. (2015). Genome-wide association study of parity in Bangladeshi women. PLoS ONE *10*, e0118488.
12. Schuh-Huerta, S.M., Johnson, N.A., Rosen, M.P., Sternfeld, B., Cedars, M.I., and Reijo Pera, R.A. (2012). Genetic variants and environmental factors associated with hormonal markers of ovarian reserve in Caucasian and African American women. Hum. Reprod. *27*, 594–608.
13. Ober, C., Elias, S., Kostyu, D.D., and Hauck, W.W. (1992). Decreased fecundability in Hutterite couples sharing HLA-DR. Am. J. Hum. Genet. *50*, 6–14.
14. Ober, C., Hyslop, T., Elias, S., Weitkamp, L.R., and Hauck, W.W. (1998). Human leukocyte antigen matching and fetal loss: results of a 10 year prospective study. Hum. Reprod. *13*, 33–38.
15. Burrows, C.K., Kosova, G., Herman, C., Patterson, K., Hartmann, K.E., Velez Edwards, D.R., Stephenson, M.D., Lynch, V.J., and Ober, C. (2016). Expression Quantitative Trait Locus Mapping Studies in Mid-secretory Phase Endometrial Cells Identifies HLA-F and TAP2 as Fecundability-Associated Genes. PLoS Genet. *12*, e1005858.
16. Dimitriadis, E., Sharkey, A.M., Tan, Y.L., Salamonsen, L.A., and Sherwin, J.R. (2007). Immunolocalisation of phosphorylated STAT3, interleukin 11 and leukaemia inhibitory factor in endometrium of women with unexplained infertility during the implantation window. Reprod. Biol. Endocrinol. *5*, 44.
17. Gellersen, B., and Brosens, J. (2003). Cyclic AMP and progesterone receptor cross-talk in human endometrium: a decidualizing affair. J. Endocrinol. *178*, 357–372.
18. Gellersen, B., Brosens, I.A., and Brosens, J.J. (2007). Decidualization of the human endometrium: mechanisms, functions, and clinical perspectives. Semin. Reprod. Med. *25*, 445–453.
19. Murakami, K., Lee, Y.H., Lucas, E.S., Chan, Y.-W., Durairaj, R.P., Takeda, S., Moore, J.D., Tan, B.K., Quenby, S., Chan, J.K.Y., et al. (2014). Decidualization induces a secretome switch in perivascular niche cells of the human endometrium. Endocrinology *155*, 4542–4553.
20. Karttunen, J.T., Lehner, P.J., Gupta, S.S., Hewitt, E.W., and Cresswell, P. (2001). Distinct functions and cooperative interaction of the subunits of the transporter associated with antigen processing (TAP). Proc. Natl. Acad. Sci. USA *98*, 7431–7436.
21. Fernandez, N., Cooper, J., Sprinks, M., AbdElrahman, M., Fiszer, D., Kurpisz, M., and Dealtry, G. (1999). A critical review of the role of the major histocompatibility complex in fertilization, preimplantation development and feto-maternal interactions. Hum. Reprod. Update *5*, 234–248.
22. GTEx Consortium (2015). Human genomics. The Genotype-Tissue Expression (GTEx) pilot analysis: multitissue gene regulation in humans. Science *348*, 648–660.
23. Melé, M., Ferreira, P.G., Reverter, F., DeLuca, D.S., Monlong, J., Sammeth, M., Young, T.R., Goldmann, J.M., Pervouchine, D.D., Sullivan, T.J., et al.; GTEx Consortium (2015). Human genomics. The human transcriptome across tissues and individuals. Science *348*, 660–665.
24. Uhlén, M., Fagerberg, L., Hallström, B.M., Lindskog, C., Oksvold, P., Mardinoglu, A., Sivertsson, Å., Kampf, C., Sjöstedt, E., Asplund, A., et al. (2015). Proteomics. Tissue-based map of the human proteome. Science *347*, 1260419.
25. Talbi, S., Hamilton, A.E., Vo, K.C., Tulac, S., Overgaard, M.T., Dosiou, C., Le Shay, N., Nezhat, C.N., Kempson, R., Lessey, B.A., et al. (2006). Molecular phenotyping of human endometrium distinguishes menstrual cycle phases and underlying biological processes in normo-ovulatory women. Endocrinology *147*, 1097–1121.
26. Goldfien, G.A., Barragan, F., Chen, J., Takeda, M., Irwin, J.C., Perry, J., Greenblatt, R.M., Smith-McCune, K.K., and Giudice, L.C. (2015). Progestin-Containing Contraceptives Alter Expression of Host Defense-Related Genes of the Endometrium and Cervix. Reprod. Sci. *22*, 814–828.
27. Pabona, J.M.P., Simmen, F.A., Nikiforov, M.A., Zhuang, D., Shankar, K., Velarde, M.C., Zelenko, Z., Giudice, L.C., and Simmen, R.C.M. (2012). Krüppel-like factor 9 and progesterone receptor coregulation of decidualizing endometrial stromal cells: implications for the pathogenesis of endometriosis. J. Clin. Endocrinol. Metab. *97*, E376–E392.
28. Davis, S., and Meltzer, P.S. (2007). GEOquery: a bridge between the Gene Expression Omnibus (GEO) and BioConductor. Bioinformatics *23*, 1846–1847.
29. Smyth, G.K. (2005). Limma: linear models for microarray data. Bioinformatics and Computational Biology Solutions. Bioinformatics and Computational Biology Solutions Using R and Bioconductor (Springer New York), pp. 397–420.
30. Gentleman, R., Carey, V., Huber, W., Irizarry, R., and Dudoit, S. (2006). Bioinformatics and computational biology solutions using R and Bioconductor (Springer New York), pp. 397–420.
31. Tamura, I., Ohkawa, Y., Sato, T., Suyama, M., Jozaki, K., Okada, M., Lee, L., Maekawa, R., Asada, H., Sato, S., et al. (2014). Genome-wide analysis of histone modifications in human endometrial stromal cells. Mol. Endocrinol. *28*, 1656–1669.
32. Lynch, V.J., Nnamani, M.C., Kapusta, A., Brayer, K., Plaza, S.L., Mazur, E.C., Emera, D., Sheikh, S.Z., Grützner, F., Bauersachs, S., et al. (2015). Ancient transposable elements transformed the uterine regulatory landscape and transcriptome during the evolution of mammalian pregnancy. Cell Rep. *10*, 551–561.
33. Delport, W., Poon, A.F.Y., Frost, S.D.W., and Kosakovsky Pond, S.L. (2010). Datamonkey 2010: a suite of phylogenetic analysis tools for evolutionary biology. Bioinformatics *26*, 2455–2457.
34. Kosakovsky Pond, S.L., and Frost, S.D. (2005). Not so different after all: a comparison of methods for detecting amino acid sites under selection. Mol. Biol. Evol. *22*, 1208–1222.
35. Wong, W.S.W., and Nielsen, R. (2004). Detecting selection in noncoding regions of nucleotide sequences. Genetics *167*, 949–958.
36. Zhang, J., Nielsen, R., and Yang, Z. (2005). Evaluation of an improved branch-site likelihood method for detecting positive selection at the molecular level. Mol. Biol. Evol. *22*, 2472–2479.
37. Haygood, R., Fedrigo, O., Hanson, B., Yokoyama, K.D., and Wray, G.A. (2007). Promoter regions of many neural- and nutrition-related genes have experienced positive selection during human evolution. Nat. Genet. *39*, 1140–1144.
38. Pond, S.L.K., Frost, S.D.W., and Muse, S.V. (2005). HyPhy: hypothesis testing using phylogenies. Bioinformatics *21*, 676–679.
39. Pybus, M., Dall'Olio, G.M., Luisi, P., Uzkudun, M., Carreño-Torres, A., Pavlidis, P., Laayouni, H., Bertranpetit, J., and Engelken, J. (2014). 1000 Genomes Selection Browser 1.0: a genome browser dedicated to signatures of natural selection in modern humans. Nucleic Acids Res. *42*, D903–D909.

40. Barragan, F., Irwin, J.C., Balayan, S., Erikson, D.W., Chen, J.C., Houshdaran, S., Piltonen, T.T., Spitzer, T.L.B., George, A., Rabban, J.T., et al. (2016). Human Endometrial Fibroblasts Derived from Mesenchymal Progenitors Inherit Progesterone Resistance and Acquire an Inflammatory Phenotype in the Endometrial Niche in Endometriosis. Biol. Reprod. *94*, 118.
41. Felker, A.M., and Croy, B.A. (2016). Uterine natural killer cell partnerships in early mouse decidua basalis. J. Leukoc. Biol., http://dx.doi.org/10.1189/jlb.1HI0515-226R.
42. Svensson, J., Jenmalm, M.C., Matussek, A., Geffers, R., Berg, G., and Ernerudh, J. (2011). Macrophages at the fetal-maternal interface express markers of alternative activation and are induced by M-CSF and IL-10. J. Immunol. *187*, 3671–3682.
43. De, M., Sanford, T., and Wood, G.W. (1993). Relationship between macrophage colony-stimulating factor production by uterine epithelial cells and accumulation and distribution of macrophages in the uterus of pregnant mice. J. Leukoc. Biol. *53*, 240–248.
44. Exley, M.A., and Boyson, J.E. (2011). Protective role of regulatory decidual γδ T cells in pregnancy. Clin. Immunol. *141*, 236–239.
45. Erlebacher, A. (2013). Mechanisms of T cell tolerance towards the allogeneic fetus. Nat. Rev. Immunol. *13*, 23–33.
46. Saito, S., Nakashima, A., Shima, T., and Ito, M. (2010). Th1/Th2/Th17 and regulatory T-cell paradigm in pregnancy. Am. J. Reprod. Immunol. *63*, 601–610.
47. Reinhard, G., Noll, A., Schlebusch, H., Mallmann, P., and Ruecker, A.V. (1998). Shifts in the TH1/TH2 balance during human pregnancy correlate with apoptotic changes. Biochem. Biophys. Res. Commun. *245*, 933–938.
48. Tagliani, E., and Erlebacher, A. (2011). Dendritic cell function at the maternal-fetal interface. Expert Rev. Clin. Immunol. *7*, 593–602.
49. Collins, M.K., Tay, C.S., and Erlebacher, A. (2009). Dendritic cell entrapment within the pregnant uterus inhibits immune surveillance of the maternal/fetal interface in mice. J. Clin. Invest. *119*, 2062–2073.
50. Mazur, E.C., Vasquez, Y.M., Li, X., Kommagani, R., Jiang, L., Chen, R., Lanz, R.B., Kovanci, E., Gibbons, W.E., and DeMayo, F.J. (2015). Progesterone receptor transcriptome and cistrome in decidualized human endometrial stromal cells. Endocrinology *156*, 2239–2253.
51. Kaya, H.S., Hantak, A.M., Stubbs, L.J., Taylor, R.N., Bagchi, I.C., and Bagchi, M.K. (2015). Roles of progesterone receptor A and B isoforms during human endometrial decidualization. Mol. Endocrinol. *29*, 882–895.
52. Li, X., Large, M.J., Creighton, C.J., Lanz, R.B., Jeong, J.-W., Young, S.L., Lessey, B.A., Palomino, W.A., Tsai, S.Y., and Demayo, F.J. (2013). COUP-TFII regulates human endometrial stromal genes involved in inflammation. Mol. Endocrinol. *27*, 2041–2054.
53. Sandelin, A., Wasserman, W.W., and Lenhard, B. (2004). ConSite: web-based prediction of regulatory elements using cross-species comparison. Nucleic Acids Res. *32*, W249–W252.
54. Mathelier, A., Fornes, O., Arenillas, D.J., Chen, C.Y., Denay, G., Lee, J., Shi, W., Shyr, C., Tan, G., Worsley-Hunt, R., et al. (2016). JASPAR 2016: a major expansion and update of the open-access database of transcription factor binding profiles. Nucleic Acids Res. *44* (D1), D110–D115.
55. Zhou, J., and Troyanskaya, O.G. (2015). Predicting effects of noncoding variants with deep learning-based sequence model. Nat. Methods *12*, 931–934.
56. Ron, D., and Habener, J.F. (1992). CHOP, a novel developmentally regulated nuclear protein that dimerizes with transcription factors C/EBP and LAP and functions as a dominant-negative inhibitor of gene transcription. Genes Dev. *6*, 439–453.
57. Jauhiainen, A., Thomsen, C., Strömbom, L., Grundevik, P., Andersson, C., Danielsson, A., Andersson, M.K., Nerman, O., Rörkvist, L., Ståhlberg, A., and Åman, P. (2012). Distinct cytoplasmic and nuclear functions of the stress induced protein DDIT3/CHOP/GADD153. PLoS ONE *7*, e33208.
58. Gao, H., and Schwartz, R.C. (2009). C/EBPzeta (CHOP/Gadd153) is a negative regulator of LPS-induced IL-6 expression in B cells. Mol. Immunol. *47*, 390–397.
59. Pomerance, M., Carapau, D., Chantoux, F., Mockey, M., Correze, C., Francon, J., and Blondeau, J.-P. (2003). CCAAT/enhancer-binding protein-homologous protein expression and transcriptional activity are regulated by 3′,5′-cyclic adenosine monophosphate in thyroid cells. Mol. Endocrinol. *17*, 2283–2294.
60. Hedrick, P.W., and Thomson, G. (1983). Evidence for balancing selection at HLA. Genetics *104*, 449–456.
61. Bubb, K.L., Bovee, D., Buckley, D., Haugen, E., Kibukawa, M., Paddock, M., Palmieri, A., Subramanian, S., Zhou, Y., Kaul, R., et al. (2006). Scan of human genome reveals no new Loci under ancient balancing selection. Genetics *173*, 2165–2177.
62. Andrés, A.M., Hubisz, M.J., Indap, A., Torgerson, D.G., Degenhardt, J.D., Boyko, A.R., Gutenkunst, R.N., White, T.J., Green, E.D., Bustamante, C.D., et al. (2009). Targets of balancing selection in the human genome. Mol. Biol. Evol. *26*, 2755–2764.
63. Cagliani, R., Riva, S., Pozzoli, U., Fumagalli, M., Comi, G.P., Bresolin, N., Clerici, M., and Sironi, M. (2011). Balancing selection is common in the extended MHC region but most alleles with opposite risk profile for autoimmune diseases are neutrally evolving. BMC Evol. Biol. *11*, 171.
64. DeGiorgio, M., Lohmueller, K.E., and Nielsen, R. (2014). A model-based approach for identifying signatures of ancient balancing selection in genetic data. PLoS Genet. *10*, e1004561.
65. Erlebacher, A. (2001). Why isn't the fetus rejected? Curr. Opin. Immunol. *13*, 590–593.
66. Medawar, P.B. (1952). Some immunological and endocrinological problems raised by the evolution of viviparity in vertebrates. Symp. Soc. Exp. Biol. *7*, 320–338.
67. Moffett, A., and Loke, Y.W. (2004). The immunological paradox of pregnancy: a reappraisal. Placenta *25*, 1–8.
68. Guerin, L.R., Prins, J.R., and Robertson, S.A. (2009). Regulatory T-cells and immune tolerance in pregnancy: a new target for infertility treatment? Hum. Reprod. Update *15*, 517–535.
69. Tirado-González, I., Barrientos, G., Freitag, N., Otto, T., Thijssen, V.L., Moschansky, P., von Kwiatkowski, P., Klapp, B.F., Winterhager, E., Bauersachs, S., and Blois, S.M. (2012). Uterine NK cells are critical in shaping DC immunogenic functions compatible with pregnancy progression. PLoS ONE *7*, e46755.
70. Nagamatsu, T., and Schust, D.J. (2010). The immunomodulatory roles of macrophages at the maternal-fetal interface. Reprod. Sci. *17*, 209–218.
71. Nancy, P., Tagliani, E., Tay, C.S., Asp, P., Levy, D.E., and Erlebacher, A. (2012). Chemokine gene silencing in decidual stromal cells limits T cell access to the maternal-fetal interface. Science *336*, 1317–1321.

72. Nagamatsu, T., Schust, D.J., Sugimoto, J., and Barrier, B.F. (2009). Human decidual stromal cells suppress cytokine secretion by allogenic CD4+ T cells via PD-1 ligand interactions. Hum. Reprod. *24*, 3160–3171.
73. Komatsu, T., Konishi, I., Mandai, M., Mori, T., Hiai, H., and Fukumoto, M. (1998). Expression of class I human leukocyte antigen (HLA) and beta2-microglobulin is associated with decidualization of human endometrial stromal cells. Hum. Reprod. *13*, 2246–2251.
74. Ober, C., Elias, S., O'Brien, E., Kostyu, D.D., Hauck, W.W., and Bombard, A. (1988). HLA sharing and fertility in Hutterite couples: evidence for prenatal selection against compatible fetuses. Am. J. Reprod. Immunol. Microbiol. *18*, 111–115.
75. Ober, C.L., Martin, A.O., Simpson, J.L., Hauck, W.W., Amos, D.B., Kostyu, D.D., Fotino, M., and Allen, F.H., Jr. (1983). Shared HLA antigens and reproductive performance among Hutterites. Am. J. Hum. Genet. *35*, 994–1004.
76. Ober, C., Aldrich, C.L., Chervoneva, I., Billstrand, C., Rahimov, F., Gray, H.L., and Hyslop, T. (2003). Variation in the HLA-G promoter region influences miscarriage rates. Am. J. Hum. Genet. *72*, 1425–1435.
77. Tan, C.Y., Ho, J.F., Chong, Y.S., Loganath, A., Chan, Y.H., Ravichandran, J., Lee, C.G., and Chong, S.S. (2008). Paternal contribution of HLA-G*0106 significantly increases risk for pre-eclampsia in multigravid pregnancies. Mol. Hum. Reprod. *14*, 317–324.
78. Loisel, D.A., Billstrand, C., Murray, K., Patterson, K., Chaiworapongsa, T., Romero, R., and Ober, C. (2013). The maternal HLA-G 1597ΔC null mutation is associated with increased risk of pre-eclampsia and reduced HLA-G expression during pregnancy in African-American women. Mol. Hum. Reprod. *19*, 144–152.
79. O'Brien, M., McCarthy, T., Jenkins, D., Paul, P., Dausset, J., Carosella, E.D., and Moreau, P. (2001). Altered HLA-G transcription in pre-eclampsia is associated with allele specific inheritance: possible role of the HLA-G gene in susceptibility to the disease. Cell. Mol. Life Sci. *58*, 1943–1949.
80. Larsen, M.H., Hylenius, S., Andersen, A.M., and Hviid, T.V. (2010). The 3′-untranslated region of the HLA-G gene in relation to pre-eclampsia: revisited. Tissue Antigens *75*, 253–261.
81. Moreau, P., Contu, L., Alba, F., Lai, S., Simoes, R., Orrù, S., Carcassi, C., Roger, M., Rabreau, M., and Carosella, E.D. (2008). HLA-G gene polymorphism in human placentas: possible association of G*0106 allele with preeclampsia and miscarriage. Biol. Reprod. *79*, 459–467.
82. Yie, S.M., Li, L.H., Xiao, R., and Librach, C.L. (2008). A single base-pair mutation in the 3′-untranslated region of HLA-G mRNA is associated with pre-eclampsia. Mol. Hum. Reprod. *14*, 649–653.
83. Aldrich, C.L., Stephenson, M.D., Karrison, T., Odem, R.R., Branch, D.W., Scott, J.R., Schreiber, J.R., and Ober, C. (2001). HLA-G genotypes and pregnancy outcome in couples with unexplained recurrent miscarriage. Mol. Hum. Reprod. *7*, 1167–1172.
84. Pfeiffer, K.A., Fimmers, R., Engels, G., van der Ven, H., and van der Ven, K. (2001). The HLA-G genotype is potentially associated with idiopathic recurrent spontaneous abortion. Mol. Hum. Reprod. *7*, 373–378.
85. Suryanarayana, V., Rao, L., Kanakavalli, M., Padmalatha, V., Raseswari, T., Deenadayal, M., and Singh, L. (2008). Association between novel HLA-G genotypes and risk of recurrent miscarriages: a case-control study in a South Indian population. Reprod. Sci. *15*, 817–824.
86. Fan, W., Li, S., Huang, Z., and Chen, Q. (2014). Relationship between HLA-G polymorphism and susceptibility to recurrent miscarriage: a meta-analysis of non-family-based studies. J. Assist. Reprod. Genet. *31*, 173–184.
87. Hylenius, S., Andersen, A.M., Melbye, M., and Hviid, T.V. (2004). Association between HLA-G genotype and risk of pre-eclampsia: a case-control study using family triads. Mol. Hum. Reprod. *10*, 237–246.
88. Cromme, F.V., Airey, J., Heemels, M.T., Ploegh, H.L., Keating, P.J., Stern, P.L., Meijer, C.J., and Walboomers, J.M. (1994). Loss of transporter protein, encoded by the TAP-1 gene, is highly correlated with loss of HLA expression in cervical carcinomas. J. Exp. Med. *179*, 335–340.
89. Van Kaer, L., Ashton-Rickardt, P.G., Ploegh, H.L., and Tonegawa, S. (1992). TAP1 mutant mice are deficient in antigen presentation, surface class I molecules, and CD4-8+ T cells. Cell *71*, 1205–1214.
90. Raghavan, M. (1999). Immunodeficiency due to defective antigen processing: the molecular basis for type 1 bare lymphocyte syndrome. J. Clin. Invest. *103*, 595–596.
91. Oliveira, C.C., Querido, B., Sluijter, M., Derbinski, J., van der Burg, S.H., and van Hall, T. (2011). Peptide transporter TAP mediates between competing antigen sources generating distinct surface MHC class I peptide repertoires. Eur. J. Immunol. *41*, 3114–3124.
92. Durgeau, A., El Hage, F., Vergnon, I., Validire, P., de Montpréville, V., Besse, B., Soria, J.C., van Hall, T., and Mami-Chouaib, F. (2011). Different expression levels of the TAP peptide transporter lead to recognition of different antigenic peptides by tumor-specific CTL. J. Immunol. *187*, 5532–5539.
93. Blanco, O., Tirado, I., Muñoz-Fernández, R., Abadía-Molina, A.C., García-Pacheco, J.M., Peña, J., and Olivares, E.G. (2008). Human decidual stromal cells express HLA-G: Effects of cytokines and decidualization. Hum. Reprod. *23*, 144–152.
94. Black, F.L., and Hedrick, P.W. (1997). Strong balancing selection at HLA loci: evidence from segregation in South Amerindian families. Proc. Natl. Acad. Sci. USA *94*, 12452–12456.
95. Markow, T., Hedrick, P.W., Zuerlein, K., Danilovs, J., Martin, J., Vyvial, T., and Armstrong, C. (1993). HLA polymorphism in the Havasupai: evidence for balancing selection. Am. J. Hum. Genet. *53*, 943–952.
96. Tan, Z., Shon, A.M., and Ober, C. (2005). Evidence of balancing selection at the HLA-G promoter region. Hum. Mol. Genet. *14*, 3619–3628.
97. Jeffreys, A.J., Ritchie, A., and Neumann, R. (2000). High resolution analysis of haplotype diversity and meiotic crossover in the human TAP2 recombination hotspot. Hum. Mol. Genet. *9*, 725–733.
98. Carter, A.J.R., and Nguyen, A.Q. (2011). Antagonistic pleiotropy as a widespread mechanism for the maintenance of polymorphic disease alleles. BMC Med. Genet. *12*, 160.
99. Anderson, C.A., Boucher, G., Lees, C.W., Franke, A., D'Amato, M., Taylor, K.D., Lee, J.C., Goyette, P., Imielinski, M., Latiano, A., et al. (2011). Meta-analysis identifies 29 additional ulcerative colitis risk loci, increasing the number of confirmed associations to 47. Nat. Genet. *43*, 246–252.

100. Franke, A., McGovern, D.P.B., Barrett, J.C., Wang, K., Radford-Smith, G.L., Ahmad, T., Lees, C.W., Balschun, T., Lee, J., Roberts, R., et al. (2010). Genome-wide meta-analysis increases to 71 the number of confirmed Crohn's disease susceptibility loci. Nat. Genet. *42*, 1118–1125.
101. Hofmann, S., Fischer, A., Nothnagel, M., Jacobs, G., Schmid, B., Wittig, M., Franke, A., Gaede, K.I., Schürmann, M., Petrek, M., et al. (2013). Genome-wide association analysis reveals 12q13.3-q14.1 as new risk locus for sarcoidosis. Eur. Respir. J. *41*, 888–900.
102. Fischer, A., Ellinghaus, D., Nutsua, M., Hofmann, S., Montgomery, C.G., Iannuzzi, M.C., Rybicki, B.A., Petrek, M., Mrazek, F., Pabst, S., et al.; GenPhenReSa Consortium (2015). Identification of Immune-Relevant Factors Conferring Sarcoidosis Genetic Risk. Am. J. Respir. Crit. Care Med. *192*, 727–736.